

Supplementary Material for:

Fundamentals of elasto-inertial particle focusing in curved microfluidic channels

Nan Xiang^{a,b*}, Xinjie Zhang^a, Qing Dai^a, Jie Cheng^a, Ke Chen^a and Zhonghua Ni^{a*}

*^aSchool of Mechanical Engineering, and Jiangsu Key Laboratory for Design and Manufacture of Micro-Nano Biomedical Instruments, Southeast University, Nanjing, 211189, China. *Electronic mails: nan.xiang@seu.edu.cn, and nzh2003@seu.edu.cn.*

^bState Key Laboratory of Fluid Power and Mechatronic Systems, Zhejiang University, Hangzhou, 310027, China

Supplementary Tables:

Table S1. Calculated dimensionless numbers (Re_c , Wi , De and El) for the experiments using 500 ppm PEO solutions.

Device i $R_i=1.1 \text{ mm}, D_h=81 \mu\text{m}, AR\sim 1/4$					Device ii $R_i=1.1 \text{ mm}, D_h=74 \mu\text{m}, AR\sim 1/3$					Device iii $R_i=1.1 \text{ mm}, D_h=64 \mu\text{m}, AR\sim 1/2$				
Q	Re_c	Wi	De	El	Q	Re_c	Wi	De	El	Q	Re_c	Wi	De	El
1	0.04	0.17	0.006	4.33	1	0.06	0.29	0.008	5.18	1	0.08	0.53	0.010	6.93
20	0.81	3.48	0.117	4.33	20	1.13	5.86	0.157	5.18	10	0.76	5.27	0.098	6.93
40	1.61	6.97	0.234	4.33	40	2.26	11.71	0.314	5.18	20	1.52	10.53	0.197	6.93
60	2.42	10.45	0.352	4.33	60	3.39	17.57	0.472	5.18	40	3.04	21.06	0.393	6.93
80	3.22	13.93	0.469	4.33	80	4.52	23.42	0.629	5.18	60	4.56	31.60	0.590	6.93
100	4.03	17.42	0.586	4.33	100	5.65	29.28	0.786	5.18	80	6.08	42.13	0.787	6.93
120	4.83	20.90	0.703	4.33	120	6.78	35.14	0.943	5.18	100	7.60	52.66	0.983	6.93
140	5.64	24.39	0.821	4.33	140	7.91	40.99	1.101	5.18	120	9.12	63.19	1.180	6.93
160	6.44	27.87	0.938	4.33	160	9.04	46.85	1.258	5.18					
180	7.25	31.35	1.055	4.33	180	10.16	52.70	1.415	5.18					
200	8.05	34.84	1.172	4.33										
220	8.86	38.32	1.290	4.33										
240	9.66	41.80	1.407	4.33										

Device I $R_i=4 \text{ mm}, D_h=79 \mu\text{m}, AR\sim 1/4$					Device II $R_i=7 \text{ mm}, D_h=79 \mu\text{m}, AR\sim 1/4$				
Q	Re_c	Wi	De	El	Q	Re_c	Wi	De	El
1	0.05	0.21	0.004	4.55	1	0.05	0.21	0.003	4.55
20	0.91	4.15	0.084	4.55	20	0.91	4.15	0.066	4.55
40	1.82	8.30	0.167	4.55	40	1.82	8.30	0.131	4.55
60	2.74	12.45	0.251	4.55	60	2.74	12.45	0.197	4.55
80	3.65	16.60	0.335	4.55	80	3.65	16.60	0.263	4.55
100	4.56	20.75	0.418	4.55	100	4.56	20.75	0.329	4.55
120	5.47	24.91	0.502	4.55	120	5.47	24.91	0.394	4.55
140	6.39	29.06	0.586	4.55	140	6.39	29.06	0.460	4.55
160	7.30	33.21	0.669	4.55	160	7.30	33.21	0.526	4.55
180	8.21	37.36	0.753	4.55	180	8.21	37.36	0.592	4.55
200	9.12	41.51	0.837	4.55	200	9.12	41.51	0.657	4.55
220	10.04	45.66	0.920	4.55	220	10.04	45.66	0.723	4.55
240	10.95	49.81	1.004	4.55	240	10.95	49.81	0.789	4.55

Table S2. Calculated dimensionless numbers (Re_c , Wi , De and El) for the control experiments with device ii using the Newtonian fluid (DI water) and the 6.8 wt% PVP solution .

Newtonian fluid (DI water)					6.8 wt% PVP solution				
Q	Re_c	Wi	De	El	Q	Re_c	Wi	De	El
10	1.76	0	0.245	0	10	0.02	0.30	0.003	15.45
20	3.52	0	0.491	0	20	0.04	0.60	0.005	15.45
30	5.29	0	0.736	0	30	0.06	0.91	0.008	15.45
40	7.05	0	0.981	0	40	0.08	1.21	0.011	15.45
50	8.81	0	1.226	0	50	0.10	1.51	0.014	15.45
60	10.57	0	1.472	0	60	0.12	1.81	0.016	15.45
70	12.33	0	1.717	0					
80	14.10	0	1.962	0					
90	15.86	0	2.207	0					
100	17.62	0	2.453	0					

Table S3. Detailed dimensions of the five-spiral channel devices employed in this work.

Device	Innermost radius R_i	Cross-sectional dimension $w \times h$	Channel aspect ratio AR	Channel loop	Distance between the adjacent channel loops	Total channel length L
i	1.1 mm	215 $\mu\text{m} \times 50 \mu\text{m}$	$\sim 1/4$	6	600 μm	8 cm
ii	1.1 mm	140 $\mu\text{m} \times 50 \mu\text{m}$	$\sim 1/3$	6	600 μm	8 cm
iii	1.1 mm	90 $\mu\text{m} \times 50 \mu\text{m}$	$\sim 1/2$	6	600 μm	8 cm
I	4 mm	190 $\mu\text{m} \times 50 \mu\text{m}$	$\sim 1/4$	3	600 μm	8 cm
II	7 mm	190 $\mu\text{m} \times 50 \mu\text{m}$	$\sim 1/4$	2	600 μm	8 cm

Supplementary Figures:

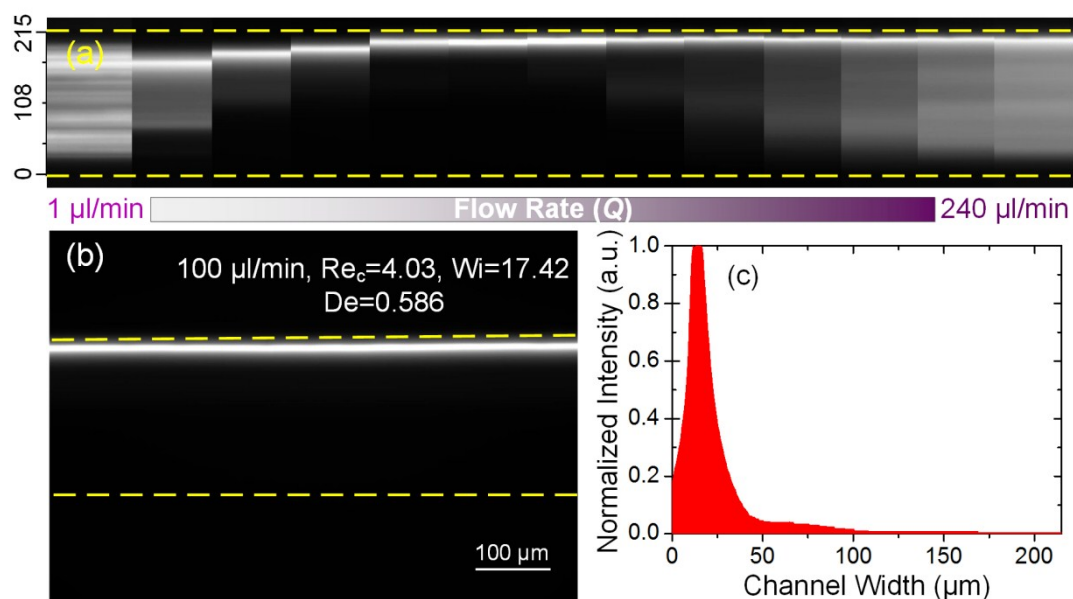


Figure S1. Focusing behaviors of particles with a smaller blockage ratio of 0.1 in device i under flow rates of 1~240 $\mu\text{l}/\text{min}$ ($Re_c=0.04\sim 9.66$, $Wi=0.17\sim 41.80$, $De=0.006\sim 1.407$). (a) Particle focusing map illustrating the particle migration with increasing flow rates. The bottom of this focusing map is the inner region of the channel and the yellow dotted lines mark the positions of the channel walls. (b) Fluorescent streak image at a flow rate of 100 $\mu\text{l}/\text{min}$ ($Re_c=4.03$, $Wi=17.42$, $De=0.586$). (c) Corresponding intensity profile across the channel width. From these two subfigures (b, c), it is found that a perfect single-line focusing can be achieved near the outer channel wall at a processing throughput of 100 $\mu\text{l}/\text{min}$.

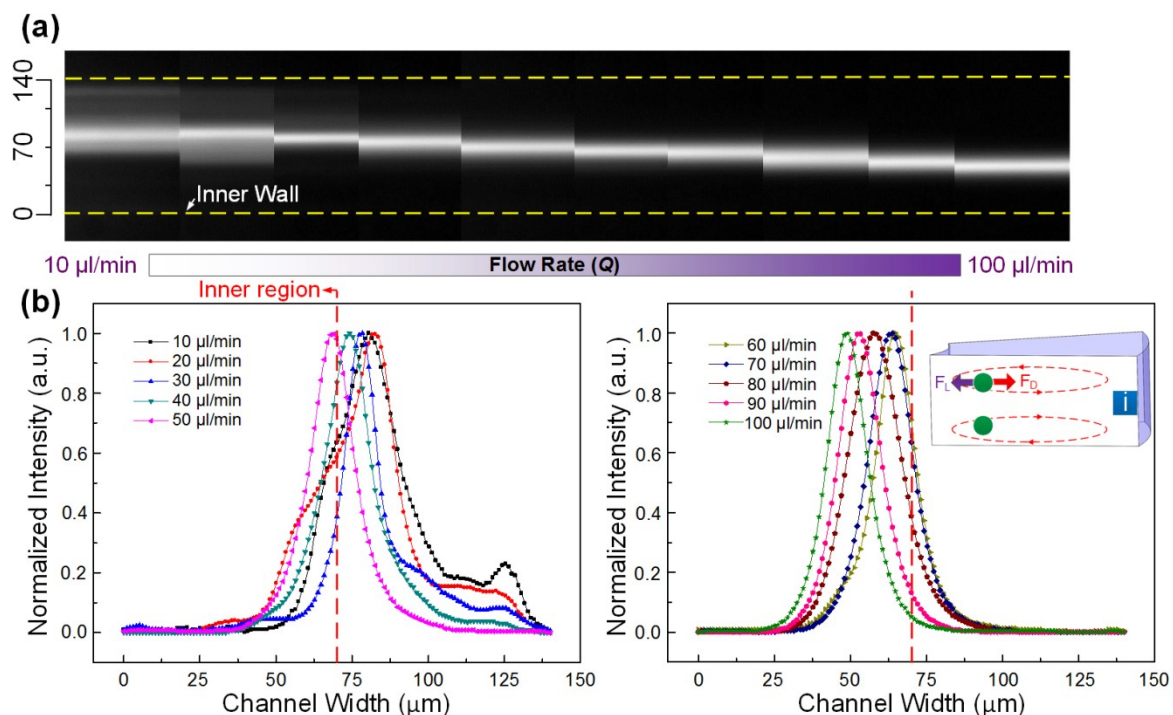


Figure S2. Particle focusing behaviors in the Newtonian fluid (DI water) under different flow rates of 10~100 $\mu\text{l}/\text{min}$ ($Re_c=1.76\sim 17.62$, $De=0.245\sim 2.453$). (a) Focusing map created by splicing the overlaid fluorescent streak images at different flow rates. The bottom of this focusing map is the inner region of the channel and the yellow dotted lines mark the positions of the channel walls. (b) Measured intensity profiles across the channel width under different flow rates. The inset (i) in the right intensity profile illustrates the schematic diagram of the force balance acting on particles. In Newtonian fluids, the particles would equilibrate in the inner channel region at high flow rates under the balance of the inertial lift force and the Dean drag force.

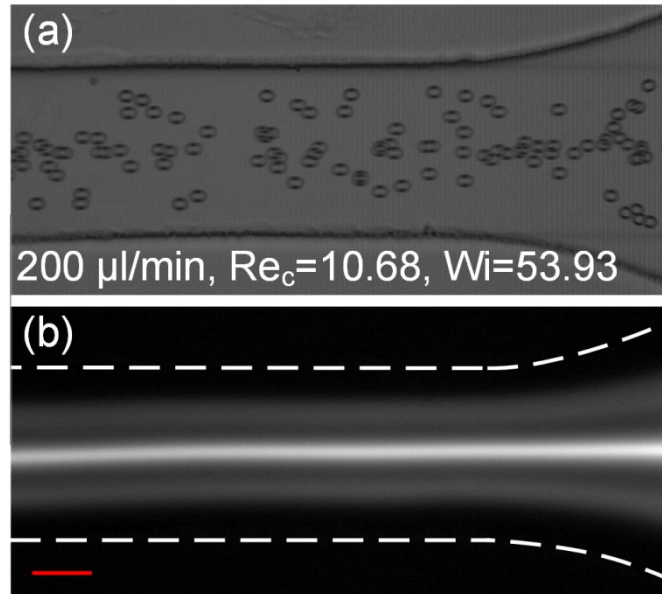


Figure S3. Observation of the particle defocusing at high flow rates ($200 \mu\text{l}/\text{min}$, $\text{Re}_c=10.68$, $\text{Wi}=53.93$) in straight channels with a cross-section of $150 \mu\text{m}$ (*width*) $\times 50 \mu\text{m}$ (*height*) and a total channel length of 4 cm. (a) Composite bright-field image. (b) Fluorescent streak image. The red scale bar is $50 \mu\text{m}$. The white dotted lines in subfigure (b) mark the positions of the channel walls.

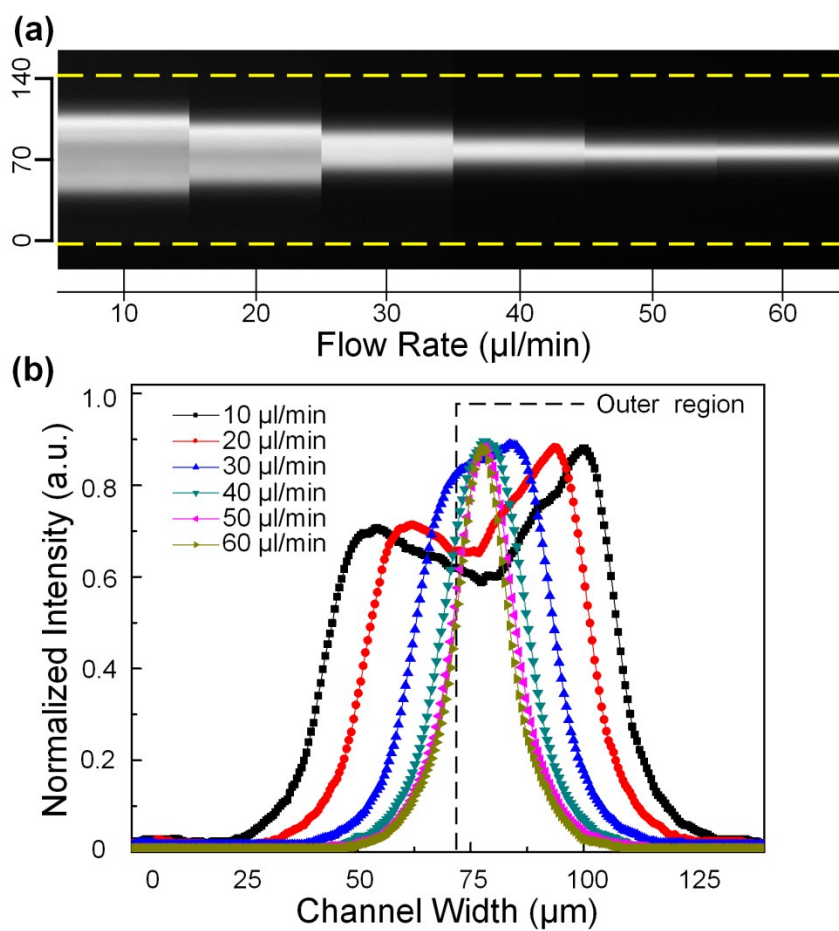


Figure S4. Particle focusing behaviors in 6.8 wt% PVP solutions with a larger El of 15.45 under different flow rates of 10~60 $\mu\text{l}/\text{min}$ ($Re_c=0.02\sim 0.12$, $Wi=0.30\sim 1.81$, $De=0.003\sim 0.016$). The maximum flow rate tested was limited to be 60 $\mu\text{l}/\text{min}$ due to the high viscosity of the prepared 6.8 wt% PVP solutions. (a) Focusing map created by splicing the overlaid fluorescent streak images at different flow rates. The bottom of this focusing map is the inner region of the channel and the yellow dotted lines mark the positions of the channel walls. (b) Measured intensity profiles across the channel width under different flow rates. As can be observed from the focusing map and the intensity profiles, a perfect single-line focusing near the channel centerline can be achieved at a flow rate larger than 30 $\mu\text{l}/\text{min}$.

Supplementary Texts:

Text S1. Derivations of force equations in the main text and the dependency of forces on parameters explored in this work.

The elastic force acting on flowing particles scales as $F_E \sim a_p^3 \nabla N_1(\dot{\gamma})$. For the Oldroyd-B model, the elastic force can be given as $F_E \sim a_p^3 \nabla N_1(\dot{\gamma}) \sim a_p^3 Wi \dot{\gamma}_c^2$.¹ We then substituted the equations of the Weissenberg number ($Wi = 2\lambda Q/hw^2$) and the characteristic shear rate ($\dot{\gamma}_c = 2Q/hw^2$) into the aforementioned equation. Therefore, a new scaling of the elastic force can be obtained as follows:

$$F_E \sim a_p^3 Wi \dot{\gamma}_c^2 = 8a_p^3 \lambda \left(\frac{Q}{hw^2} \right)^3.$$

For $a_p/h \ll 1$, the inertial lift force acting on particles can be expressed as $F_L \sim \rho U^2 a_p^4 / D_h^2$.² The average fluid velocity can be calculated as $U = Q/hw$, and the hydraulic diameter is $D_h = 2wh/(w+h)$. Substituting the definition of U and D_h into the scaling of the inertial lift force yields

$$F_L \sim \rho U^2 a_p^4 / D_h^2 = \frac{1}{4} \rho Q^2 a_p^4 \frac{(w+h)^2}{(wh)^4}.$$

Similarly, the scaling of the Dean drag force can be written as:³

$$F_D \sim \rho U^2 a_p D_h^2 R^{-1} = \frac{4\rho Q^2 a_p}{R(w+h)^2}.$$

On the basis of the above derivations, the dependency of forces on parameters explored in this work (i.e., flow rate (Q), channel dimensions, particle blockage ratio (α), channel radius (R) and fluid rheology) can be summarized as follows:

	Flow rate (Q)	Channel dimensions (h and w)	Particle blockage ratio (α)	Channel radius (R)	Fluid rheology
Elastic force (F_E)	$F_E \sim Q^3$	$\frac{1}{F_E \sim h^3 w^6}$	$F_E \sim \alpha^3$	<i>unrelated</i>	$F_E \sim \lambda$

Inertial lift force (F_L)	$F_L \sim Q^2$	$\frac{(w+h)^2}{F_L \sim (wh)^4}$	$F_L \sim \alpha^4$	<i>unrelated</i>	<i>unrelated</i>
Dean drag force (F_D)	$F_D \sim Q^2$	$\frac{1}{F_D \sim (w+h)^2}$	$F_D \sim \alpha$	$F_D \sim R^{-1}$	<i>unrelated</i>

References

1. X. Lu, L. Zhu, R.-m. Hua and X. Xuan, *Applied Physics Letters*, 2015, **107**, 264102.
2. H. Amini, W. Lee and D. Di Carlo, *Lab on a Chip*, 2014, **14**, 2739-2761.
3. D. Di Carlo, D. Irimia, R. G. Tompkins and M. Toner, *Proceedings of the National Academy of Sciences of the United States of America*, 2007, **104**, 18892-18897.